

# Dynamic Modeling and Adaptive Neural-Fuzzy Control for Nonholonomic Mobile Manipulators Moving on a Slope

Yugang Liu and Yangmin Li\*

**Abstract:** This paper addresses dynamic modeling and task-space trajectory following issues for nonholonomic mobile manipulators moving on a slope. An integrated dynamic modeling method is proposed considering nonholonomic constraints and interactive motions. An adaptive neural-fuzzy controller is presented for end-effector trajectory following, which does not rely on precise a priori knowledge of dynamic parameters and can suppress bounded external disturbances. Effectiveness of the proposed algorithm is verified through simulations.

**Keywords:** Adaptive control, mobile manipulator, neural-fuzzy control, nonholonomic.

## 1. INTRODUCTION

Intelligent and autonomous mobile manipulators have attracted attentions from numerous scholars in recent years since they have wide applications. A nonholonomic mobile manipulator is normally composed of a  $m$ -wheeled nonholonomic mobile platform and a  $n$ -DOF onboard manipulator. This combination extends workspace of the entire robot drastically. However, dynamic modeling and trajectory following become difficult to achieve due to their interactive motions. Also moving on a slope makes them even more complex.

Neural networks (NNs) and fuzzy logic systems have been widely used for robotic control because they are universal approximators. As a combination of these two techniques, neural-fuzzy systems can make good use of both sensory numerical data and expert linguistic information. Unlike conventional NNs, the proposed adaptive neural-fuzzy controller (ANFC) does not need off-line training and can incorporate expert experience easily.

In related research works, the authors investigated vibration control for modular manipulators and trajectory tracking control of mobile manipulators exploiting back propagation NNs [1,2]. Real experiment for mobile manipulators using NN control was approached [3]. Dynamic characteristics between the mobile platform and the manipulator were studied

in [4]. A series of RBF NNs were adopted for dynamic modeling and an adaptive controller was devised for task-space trajectory following of robotic manipulators [5]. A multi-layer NN controller, which did not need off-line learning was designed for rigid robotic control [6]. A fuzzy-Gaussian NN controller was proposed for trajectory tracking of mobile robots [7]. A robust fuzzy logic controller was devised for a robotic manipulator with uncertainties [8].

This paper is organized in five parts with the following part establishing the dynamic model. In Section 3, the ANFC is presented in task space and the systematic stable characteristic is verified. A simulation is carried out for a real mobile manipulator in Section 4. Finally, some concluding remarks are given in Section 5.

## 2. INTEGRATED DYNAMIC MODELING

In this paper, a 3-wheeled nonholonomic mobile manipulator is analyzed, as shown in Fig. 1. The coordinate systems are defined as follows:  $O_B X_B Y_B Z_B$  forms an inertial base frame and  $O_S X_S Y_S Z_S$  is a frame fixed on the slope; while  $O_m X_m Y_m Z_m$  is a frame mounted on the mobile platform. In frame  $O_m X_m Y_m Z_m$ ,  $O_m$  is selected at the midpoint of the line segment connecting the two fixed wheel centers; and  $Y_m$  is along the coaxial-line of the two fixed wheels. The heading angle  $\phi_m$  determines posture of the mobile platform.  $\phi_L$  and  $\phi_R$  are rotating angles of the left and right wheel;  $d_m$ ,  $r_f$ ,  $l_G$ ,  $h_m$  and  $\theta_s$  are all constants as marked in Fig. 1.

Considering the mobile manipulator as an integrated structure, we can obtain the transformation matrix of the 1<sup>st</sup> link with respect to frame

Manuscript received October 28, 2004; revised September 20, 2005; accepted January 16, 2006. Recommended by Editorial Board member Jin Young Choi under the direction of Editor Keum-Shik Hong.

Yugang Liu and Yangmin Li are with the Faculty of Science and Technology, University of Macau, Av. Padre Tomàs Pereira S.J., Taipa, Macao S.A.R., P. R. China (e-mails: {ya27401, ymli}@umac.mo).

\* Corresponding author.

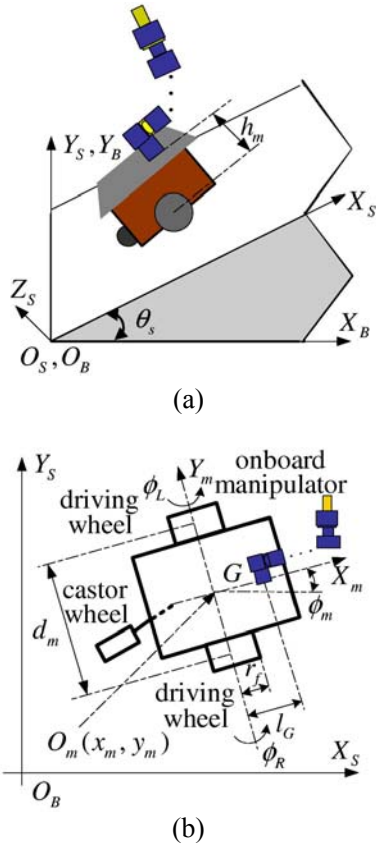


Fig. 1. Motion of a mobile manipulator on a slope.

$O_B X_B Y_B Z_B$ :

$${}^B_0 T = \begin{bmatrix} c_s & 0 & -s_s & 0 \\ 0 & 1 & 0 & 0 \\ s_s & 0 & c_s & 0 \\ 0 & 0 & 0 & 1 \end{bmatrix} \cdot \begin{bmatrix} c_m & -s_m & 0 & x_m + l_g \cdot c_m \\ s_m & c_m & 0 & y_m + l_g \cdot s_m \\ 0 & 0 & 1 & z_m + h_m \\ 0 & 0 & 0 & 1 \end{bmatrix}, \quad (1)$$

where  $s_s = \sin \theta_s$ ,  $c_s = \cos \theta_s$ ,  $s_m = \sin \phi_m$ ,  $c_m = \cos \phi_m$ .

According to Denavit-Hartenberg notation, transformation matrix of the  $i^{\text{th}}$  link with respect to  $O_B X_B Y_B Z_B$  can be derived. Furthermore, the positions  $(p_x, p_y, p_z)$  and posture vectors  $(\vec{n}, \vec{o}, \vec{a})$  of the end-effector can also be obtained. The posture can also be determined by 3 independent parameters with  $Z-Y-Z$  Euler angles  $(\phi, \theta, \psi)$  [9]

$$\begin{cases} \phi = \arctan 2(a_y, a_x), \\ \psi = \arctan 2(o_z, -n_z), \\ \theta = \arctan 2(a_x \cdot \cos \phi + a_y \cdot \sin \phi, a_z). \end{cases} \quad (2)$$

Define general coordinates of the mobile platform as  $\xi = [x_m \ y_m \ \phi_m \ \phi_L \ \phi_R]^T$ ; on the assumption of low speeds, nonholonomic constraints of the mobile

platform can be given by [10]:

$$A(\xi) \cdot S(\xi) = 0_{3 \times 2}, \quad (3)$$

where  $A(\xi)$  and  $S(\xi)$  can be detailed by

$$A(\xi) = \begin{bmatrix} c_m & s_m & \frac{d_m}{2} & -r_f & 0 \\ c_m & s_m & \frac{d_m}{2} & 0 & -r_f \\ s_m & -c_m & 0 & 0 & 0 \end{bmatrix},$$

$$S(\xi) = \begin{bmatrix} \frac{r_f \cdot c_m}{2} & \frac{r_f \cdot s_m}{2} & -\frac{r_f}{d_m} & 1 & 0 \\ \frac{r_f \cdot c_m}{2} & \frac{r_f \cdot s_m}{2} & \frac{r_f}{d_m} & 0 & 1 \end{bmatrix}^T. \quad (4)$$

Let  $q = [\phi_L \ \phi_R \ q_1 \ \dots \ q_n]^T$ ,  $\zeta = [x_m \ y_m \ \phi_m \ q^T]^T$ ,  $x = [p_x \ p_y \ p_z \ \phi \ \theta \ \psi]^T$ , then we can obtain:

$$J = \frac{\partial x}{\partial q} = \frac{\partial x}{\partial \zeta} \cdot \begin{bmatrix} S(\xi) & 0_{5 \times n} \\ 0_{n \times 2} & I_{n \times n} \end{bmatrix}. \quad (5)$$

In short  $J = \frac{\partial x}{\partial \zeta} \cdot \bar{S}$ ; here  $J$  is the Jacobian matrix.

Let  $L$  be the Lagrange function, then the constrained dynamics can be determined by

$$\frac{d}{dt} \left( \frac{\partial L}{\partial \dot{\zeta}} \right)^T - \left( \frac{\partial L}{\partial \zeta} \right)^T = B(\zeta) \cdot (\tau + J^T \cdot F_{ext}) + C(\zeta) \cdot \lambda, \quad (6)$$

where  $B = [0_{(n+2) \times 3} \ I_{(n+2) \times (n+2)}]^T \in \mathfrak{R}^{(n+5) \times (n+2)}$ ,  $C = [A(\xi) \ 0_{3 \times n}]^T \in \mathfrak{R}^{(n+5) \times 3}$ ;  $F_{ext} \in \mathfrak{R}^6$  is a vector of external forces or moments added to the end-effector;  $\tau = [\tau_L \ \tau_R \ \tau_1 \ \dots \ \tau_n]^T \in \mathfrak{R}^{(n+2)}$  is the driving torque vector;  $\lambda = [\lambda_1 \ \lambda_2 \ \lambda_3]^T$  are Lagrange multipliers.

(6) can be rewritten as:

$$M \cdot \ddot{\zeta} + V \cdot \dot{\zeta} + G = B \cdot (\tau + J^T \cdot F_{ext}) + C \cdot \lambda, \quad (7)$$

where  $M$ ,  $V$  and  $G$  represent the inertial matrix, the centripetal and coriolis matrix, and the gravitational force vector respectively.

From (5) we can obtain:

$$\dot{\zeta} = \bar{S} \cdot J^{-1} \cdot \dot{x}. \quad (8)$$

Substituting (8) and its derivative into (7) and left multiplying  $J^{-T} \cdot \bar{S}^T$ , yields:

$$\bar{M} \cdot \ddot{x} + \bar{V} \cdot \dot{x} + \bar{G} = \bar{\tau}, \quad (9)$$

where  $\bar{M} = J^{-T} \bar{S}^T M \bar{S} J^{-1}$ ,  $\bar{\tau} = J^{-T} \bar{S}^T B(\tau + J^T F_{ext})$ ,  $\bar{V} = J^{-T} \bar{S}^T (M \dot{\bar{S}} J^{-1} + M \bar{S} \dot{j}^{-1} + V \bar{S} J^{-1})$ ,  $\bar{G} = J^{-T} \bar{S}^T G$ ; the term  $J^{-T} \bar{S}^T C = 0$  is eliminated.

**Remark 1:** The following properties hold for (9):

- 1)  $\bar{M}^T = \bar{M} > 0$ .
- 2) for any  $\gamma \in \mathfrak{R}^6$ ,  $\gamma^T \cdot (\dot{\bar{M}} - 2\dot{\bar{V}}) \cdot \gamma = 0$ .
- 3)  $\bar{M}$ ,  $\bar{V}$  and  $\bar{G}$  are all bounded if  $J$  keeps nonsingular.

### 3. ADAPTIVE NEURAL-FUZZY CONTROLLER DESIGN

It is verified that multiple input single output (MISO) fuzzy logic system with center average defuzzifier, product-inference rule and singleton fuzzifier, and Gaussian membership function can uniformly approximate any nonlinear functions over a compact set  $U \in \mathfrak{R}^n$  to any degree of accuracy [11]. If the fuzzy logic system described above is realized by a NN, we can obtain a NFS, as shown in Fig. 2.

The output of a MISO NFS in Fig. 2 is

$$f_{NFS} = \frac{\sum_{j=1}^{N_r} \left\{ w_j \cdot \prod_{i=1}^{N_i} \left\{ \exp \left[ - \left( \frac{x_i - \varpi_{ji}}{\sigma_{ji}} \right)^2 \right] \right\} \right\}}{\sum_{j=1}^{N_r} \left\{ \prod_{i=1}^{N_i} \exp \left[ - \left( \frac{x_i - \varpi_{ji}}{\sigma_{ji}} \right)^2 \right] \right\}}, \quad (10)$$

where  $x_i$  is the  $i^{th}$  input variable;  $w_j$  denotes a real weight of the consequent part;  $i = 1, 2, \dots, N_i$ , and  $j = 1, 2, \dots, N_r$ , with  $N_i$  and  $N_r$  denoting the number of input variables and rules respectively.  $\varpi_{ji}$  and  $\sigma_{ji}$  are the mean and standard derivations of the Gaussian membership functions.

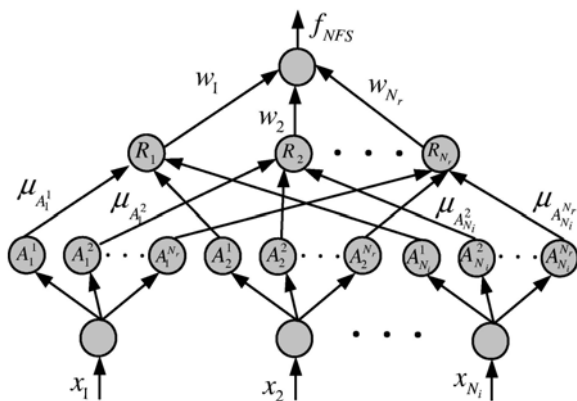


Fig. 2. A multiple input single output NFS.

The desired trajectory, velocity, and acceleration are supposed to be  $x_d(t)$ ,  $\dot{x}_d(t)$ , and  $\ddot{x}_d(t)$ . To avoid measuring accelerations, the error system can be defined by

$$\begin{aligned} e(t) &= x(t) - x_d(t), \\ \dot{x}_\gamma(t) &= \dot{x}_d(t) - \Lambda \cdot e(t), \\ \gamma(t) &= \dot{e}(t) + \Lambda \cdot e(t), \end{aligned} \quad (11)$$

where  $\gamma(t)$  is the well known tracking error measure;  $\Lambda \in \mathfrak{R}^{6 \times 6}$  is a constant, positive definite matrix.

Substituting (11) into (9), yields

$$\bar{M} \cdot \dot{\gamma}(t) + \bar{V} \cdot \gamma(t) + \bar{M} \cdot \ddot{x}_\gamma + \bar{V} \cdot \dot{x}_\gamma + \bar{G} = \bar{\tau}. \quad (12)$$

Define  $g(\zeta, \dot{\zeta}, \dot{x}_\gamma, \ddot{x}_\gamma) = \bar{M} \cdot \ddot{x}_\gamma + \bar{V} \cdot \dot{x}_\gamma + \bar{G} \in \mathfrak{R}^6$ .

From (11) and Remark 1, we can see that  $g$  is bounded and belongs to a compact set as long as  $J$  keeps nonsingular. Therefore, according to the universal approximation theory mentioned above, each element of  $g$  can be approximated by a MISO NFS in the form of (10). Furthermore, from the nonholonomic velocity constraints and the error system defined above, inputs to these NFS can be selected as  $\chi =$

$$\left[ \zeta^T \quad \dot{q}^T \quad x_d^T \quad \dot{x}_d^T \quad \ddot{x}_d^T \right]^T. \text{ Then,}$$

$$g_k(\chi) = f_{NFS}(\chi, \varpi_k, \sigma_k, w_k) + \varepsilon_k(\chi), \quad (13)$$

where  $g_k$  is the  $k^{th}$  element of  $g$ ;  $\varpi_k, \sigma_k \in \mathfrak{R}^{N_r \times N_i}$ , and  $w_k \in \mathfrak{R}^{N_r}$  are adjustable parameter matrices for the NFS;  $\varepsilon_k(\chi)$  is the approximated error;  $k = 1, 2, \dots, 6$ .

Assume  $\chi \in [\underline{\chi}, \bar{\chi}]$ ,  $g \in [\underline{g}, \bar{g}]$ , if we know the system very well, then the adjustable parameters can be initialized according to human experience. However, if we does not have any apriori knowledge of the system, the adjustable parameters can be initialized in such a way that the centroids are scattered evenly in the fuzzy sets, i.e.,

$$\begin{aligned} \varpi_{kji0} &= \underline{\chi}_i + j \cdot \frac{\bar{\chi}_i - \underline{\chi}_i}{N_r}, & \sigma_{kji0} &= \frac{\bar{\chi}_i - \underline{\chi}_i}{N_r}, \\ w_{kj0} &= \underline{g}_k + j \cdot \frac{\bar{g}_k - \underline{g}_k}{N_r}. \end{aligned} \quad (14)$$

Let  $\hat{\varpi}_k$ ,  $\hat{\sigma}_k$ , and  $\hat{w}_k$  be estimates of  $\varpi_k$ ,  $\sigma_k$ , and  $w_k$  respectively. Taking the Taylor series expansions of  $g_{NFSk} = f_{NFS}(\chi, \varpi_k, \sigma_k, w_k)$  around  $\hat{g}_{NFSk} = f_{NFS}(\chi, \hat{\varpi}_k, \hat{\sigma}_k, \hat{w}_k)$ , we can obtain

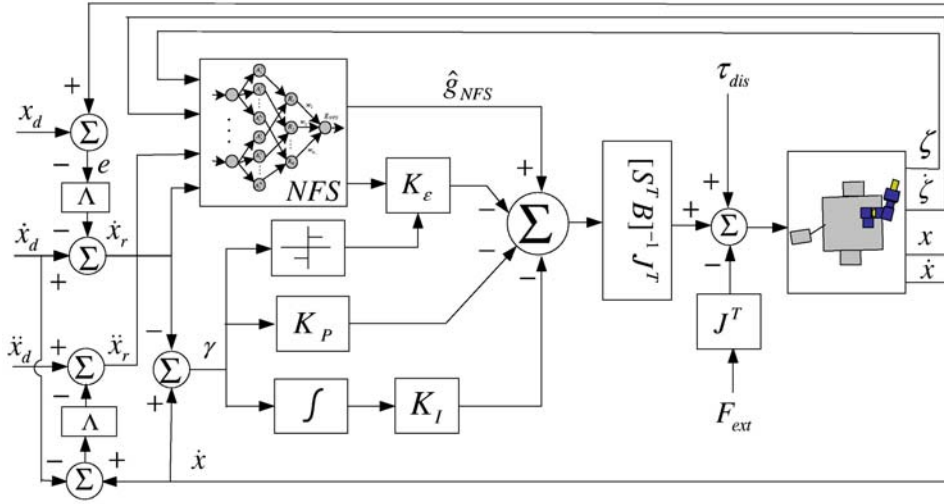


Fig. 3. An adaptive neural-fuzzy controller.

$$\begin{aligned} \tilde{g}_{NFSk} &= \sum_{j=1}^{N_r} \left\{ \sum_{i=1}^{N_i} \left[ O(\tilde{\omega}_{kji}^2) + O(\tilde{\sigma}_{kji}^2) \right] + O(\tilde{w}_{kj}^2) \right\} \\ &+ \sum_{j=1}^{N_r} \left\{ \sum_{i=1}^{N_i} \left[ \frac{\partial \hat{g}_{NFSk}}{\partial \omega_{kji}} \tilde{\omega}_{kji} + \frac{\partial \hat{g}_{NFSk}}{\partial \sigma_{kji}} \tilde{\sigma}_{kji} \right] + \frac{\partial \hat{g}_{NFSk}}{\partial w_{kj}} \tilde{w}_{kj} \right\}, \end{aligned} \quad (15)$$

where  $\tilde{g}_{NFSk} = g_{NFSk} - \hat{g}_{NFSk}$ ,  $\tilde{\omega}_{kji} = \omega_{kji} - \hat{\omega}_{kji}$ ,  $\tilde{\sigma}_{kji} = \sigma_{kji} - \hat{\sigma}_{kji}$ ,  $\tilde{w}_{kj} = w_{kj} - \hat{w}_{kj}$ ;  $O(\tilde{\omega}_{kji}^2)$ ,  $O(\tilde{\sigma}_{kji}^2)$  and  $O(\tilde{w}_{kj}^2)$  are higher-order terms;  $\frac{\partial \hat{g}_{NFSk}}{\partial \omega_{kji}}$ ,  $\frac{\partial \hat{g}_{NFSk}}{\partial \sigma_{kji}}$  and  $\frac{\partial \hat{g}_{NFSk}}{\partial w_{kj}}$  can be detailed as follows

$$\begin{aligned} \frac{\partial \hat{g}_{NFSk}}{\partial w_{kj}} &= \frac{\prod_{i=1}^{N_i} \left\{ \exp \left[ -\left( \frac{\chi_i - \hat{\omega}_{kji}}{\hat{\sigma}_{kji}} \right)^2 \right] \right\}}{\sum_{j=1}^{N_r} \left\{ \prod_{i=1}^{N_i} \exp \left[ -\left( \frac{\chi_i - \hat{\omega}_{kji}}{\hat{\sigma}_{kji}} \right)^2 \right] \right\}}, \\ \frac{\partial \hat{g}_{NFSk}}{\partial \omega_{kji}} &= \frac{2 \cdot (\chi_i - \hat{\omega}_{kji}) \cdot (\hat{w}_{kj} - \hat{g}_{NFSk})}{\hat{\sigma}_{kji}^2} \cdot \frac{\partial \hat{g}_{NFSk}}{\partial w_{kj}}, \\ \frac{\partial \hat{g}_{NFSk}}{\partial \sigma_{kji}} &= \frac{2 \cdot (\chi_i - \hat{\omega}_{kji}) \cdot (\hat{w}_{kj} - \hat{g}_{NFSk})}{\hat{\sigma}_{kji}^3} \cdot \frac{\partial \hat{g}_{NFSk}}{\partial w_{kj}}. \end{aligned} \quad (16)$$

The ANFC presented in this paper is given by (17), and a control system diagram is shown in Fig. 3.

$$\begin{aligned} \tau &= (\bar{S}^T \cdot B)^{-1} \cdot J^T \cdot \{ \hat{g}_{NFS} - K_e \cdot \text{sgn}(\gamma) \\ &- K_P \cdot \gamma - K_I \cdot \int_0^t \gamma(t) dt \} - J^T \cdot F_{ext}, \end{aligned} \quad (17)$$

where  $K_p, K_I \in \mathfrak{R}^{6 \times 6}$  are respectively proportional and integral gain matrices;  $K_e = \text{diag} \{ k_{\varepsilon 1} \ \dots \ k_{\varepsilon 6} \}$ , and

$$k_{\varepsilon k} \geq |\varepsilon_k| + \left| \sum_{j=1}^{N_r} \left\{ \sum_{i=1}^{N_i} \left[ O(\tilde{\omega}_{kji}^2) + O(\tilde{\sigma}_{kji}^2) \right] + O(\tilde{w}_{kj}^2) \right\} \right|.$$

Substituting (17) into (12), and considering (9), (13) at the same time, yields

$$\begin{aligned} \bar{M} \cdot \dot{\gamma} + \bar{V} \cdot \gamma + K_P \cdot \gamma + K_I \cdot \int_0^t \gamma(t) dt \\ + g_{NFS} - \hat{g}_{NFS} + \varepsilon + K_e \cdot \text{sgn}(\gamma) = 0, \end{aligned} \quad (18)$$

where  $\varepsilon = [\varepsilon_1 \ \dots \ \varepsilon_6]^T$ .

**Theorem 1:** If  $K_P > 0$ ,  $K_I^T = K_I > 0$ , the close-loop system in (18) is asymptotically stable under the following parameter adaptation laws given by (19). The error signals are convergent along with time, i.e.,  $e(t)$ ,  $\dot{e}(t) \rightarrow 0$ , as  $t \rightarrow +\infty$ .

$$\begin{aligned} \dot{\hat{\omega}}_{kji} &= -\Gamma_{\omega_{kji}} \cdot \gamma_k \cdot \frac{\partial \hat{g}_{NFSk}}{\partial \omega_{kji}}, \\ \dot{\hat{\sigma}}_{kji} &= -\Gamma_{\sigma_{kji}} \cdot \gamma_k \cdot \frac{\partial \hat{g}_{NFSk}}{\partial \sigma_{kji}}, \\ \dot{\hat{w}}_{kj} &= -\Gamma_{w_{kj}} \cdot \gamma_k \cdot \frac{\partial \hat{g}_{NFSk}}{\partial w_{kj}}, \end{aligned} \quad (19)$$

where  $\Gamma_{\omega_{kji}}, \Gamma_{\sigma_{kji}}$  and  $\Gamma_{w_{kj}}$  are all positive constants.

**Proof:** Consider the following nonnegative Lyapunov candidate:

$$\begin{aligned} V_S &= \frac{1}{2} \gamma^T \bar{M} \gamma + \frac{1}{2} \left[ \int_0^t \gamma(t) dt \right]^T K_I \left[ \int_0^t \gamma(t) dt \right] \\ &+ \frac{1}{2} \cdot \sum_{k=1}^6 \sum_{j=1}^{N_r} \left\{ \sum_{i=1}^{N_i} \left( \frac{\tilde{\omega}_{kji}^2}{\Gamma_{\omega_{kji}}} + \frac{\tilde{\sigma}_{kji}^2}{\Gamma_{\sigma_{kji}}} \right) + \frac{\tilde{w}_{kj}^2}{\Gamma_{w_{kj}}} \right\} \geq 0. \end{aligned} \quad (20)$$

The time derivative of Lyapunov candidate is

$$\begin{aligned} \dot{V}_S = & \gamma^T \left\{ \bar{M} \cdot \dot{\gamma} + K_I \left[ \int_0^t \gamma(t) dt \right] \right\} + \frac{1}{2} \gamma^T \dot{\bar{M}} \gamma \\ & + \sum_{k=1}^6 \sum_{j=1}^{N_r} \left[ \sum_{i=1}^{N_i} \left( \frac{\tilde{\omega}_{kji} \dot{\tilde{\omega}}_{kji}}{\Gamma_{\varpi_{kji}}} + \frac{\tilde{\sigma}_{kji} \dot{\tilde{\sigma}}_{kji}}{\Gamma_{\sigma_{kji}}} \right) + \frac{\tilde{w}_{kj} \dot{\tilde{w}}_{kj}}{\Gamma_{w_{kj}}} \right]. \end{aligned} \quad (21)$$

Substituting (18) into (21) and considering Remark 1 at the same time, yield

$$\begin{aligned} \dot{V}_S = & -\gamma^T K_P \gamma - \gamma^T \left[ \tilde{g}_{NFS} + \varepsilon + K_\varepsilon \cdot \text{sgn}(\gamma) \right] \\ & + \sum_{k=1}^6 \sum_{j=1}^{N_r} \left[ \sum_{i=1}^{N_i} \left( \frac{\tilde{\omega}_{kji} \dot{\tilde{\omega}}_{kji}}{\Gamma_{\varpi_{kji}}} + \frac{\tilde{\sigma}_{kji} \dot{\tilde{\sigma}}_{kji}}{\Gamma_{\sigma_{kji}}} \right) + \frac{\tilde{w}_{kj} \dot{\tilde{w}}_{kj}}{\Gamma_{w_{kj}}} \right]. \end{aligned} \quad (22)$$

Notice that  $\dot{\tilde{\omega}}_{kji} = -\dot{\hat{\omega}}_{kji}$ ,  $\dot{\tilde{\sigma}}_{kji} = -\dot{\hat{\sigma}}_{kji}$ ,  $\dot{\tilde{w}}_{kj} = -\dot{\hat{w}}_{kj}$ , substituting (15), (19) into (22) and considering (17) at the same time, yield

$$\dot{V}_S \leq -\gamma^T \cdot K_P \cdot \gamma \leq 0. \quad (23)$$

From (20), (23), we can see that  $V_S$  is a Lyapunov function. Furthermore,  $V_S = 0$  and  $\dot{V}_S = 0$  have only one solution  $\gamma = 0$ . According to LaSalle's theorem, we can conclude that the system is asymptotically stable and  $\gamma \rightarrow 0$  as  $t \rightarrow \infty$ .

Define  $\|x\|_p = \left( \int_0^{+\infty} |x(t)|^p dt \right)^{\frac{1}{p}}$  p-norm for  $x(t)$

and  $\ell_p = \left\{ x(t) \in \mathfrak{R}^n : \|x\|_p < \infty \right\}$  the functional space over which the signal p-norm exists. From (20),(23), we can conclude that  $\gamma(t) \in \ell_2 \cap \ell_\infty$ . From (11), we can see that  $e(t) \in \ell_2 \cap \ell_\infty$ ,  $\dot{e}(t) \in \ell_2$  and in fact  $e(t) \rightarrow 0$  as  $t \rightarrow \infty$ . Since  $\dot{V}_S \leq 0$ ,  $V_S \in \ell_\infty$ , which implies that  $\tilde{\omega}_{kji}, \tilde{\sigma}_{kji}, \tilde{w}_{kj} \in \ell_\infty$ , if  $J$  keeps nonsingular,  $g$  will be bounded and  $\varpi_{kji}$ ,  $\sigma_{kji}$ ,  $w_{kj} \in \ell_\infty$ , so,  $\hat{\omega}_{kji}, \hat{\sigma}_{kji}, \hat{w}_{kj} \in \ell_\infty$  and  $\hat{g}$  is bounded. It is obvious that the higher-order terms in (15) are bounded, so  $K_\varepsilon \in \ell_\infty$ . Then, from (18), we can see that  $\dot{\gamma}(t) \in \ell_\infty$ . Since,  $\gamma(t) \in \ell_2 \cap \ell_\infty$  and  $\dot{\gamma}(t) \in \ell_\infty$ , we can conclude that  $\gamma(t) \rightarrow 0$  as  $t \rightarrow \infty$ , which is followed by  $\dot{e}(t) \rightarrow 0$ . This is the end of proof.  $\square$

#### 4. SIMULATION RESULTS

In this simulation, the mobile manipulator is composed of a 3-wheeled nonholonomic mobile

platform, called "Pioneer 3-DXe", and a 4-DOF onboard manipulator, named "POWER-CUBE".

In this simulation, each element of  $g$  is approximated by a NFS in rules number of  $N_r = 200$ ; and all the adjustable parameters are initialized according to Eq. 14. The gradient angle of the slope is supposed to be  $30^\circ$ . To ensure the system far away from singularities, a singularity free trajectory is predefined, as shown in Fig. 4(a). Simulation time interval is chosen as 12 seconds. Gain matrices and constants are selected as

$$\begin{aligned} K_P = & \text{diag} \{100\}, & \Gamma_{\sigma_{kji}} = & 0.1, \\ K_I = & \text{diag} \{10\}, & \Gamma_{\varpi_{kji}} = & 0.1, \\ \Lambda = & \text{diag} \{2\}, & \Gamma_{w_{kj}} = & 0.2. \end{aligned} \quad (24)$$

To examine the disturbance suppression characteristics of the controller, a series of disturbance torques are applied which are sampled from band-limited white noise, as shown in Fig. 4(b); and an external force  $F_{ext} = 20N$  is added to the end-effector along  $O_B X_B$  at the time instant  $t = 2s$ .

Fig. 4(a) gives the desired and controlled locus of the end-effector; tracking position and Euler angular errors are shown in Figs. 4(c)-4(d) respectively; Figs. 4(e)-4(f) show tracking linear and Euler angular velocity errors accordingly; time-variant torques will not be presented here because of page limitations. From these figures, we can see that the ANFC has a strong disturbance suppression ability. Small errors can be eliminated soon.

**Remark 2:** The ANFC is designed in task-space directly, so calculation of inverse Jacobian can be avoided. However, this scheme needs some task-space information, such as  $x$  and  $\dot{x}$ , which is difficult to measure. In this case, the task-space information is calculated by forward kinematics and differential kinematics respectively. Another solution is to construct a vision-based control system. However, such a system will not be widely used in practice until a very powerful but not too expensive camera with high speed data processing ability appears. This paper aims to present a theoretical analysis method and the experiment will be carried out in our future study. Furthermore, the combination of a mobile platform with a manipulator make the robot easy to overturn in case of moving on a slope. Such a problem can be solved by adding extra balance weights or by adjusting self-motions for redundant mobile manipulators [12].

#### 5. CONCLUSIONS

This paper investigates the trajectory following problem for nonholonomic mobile manipulators

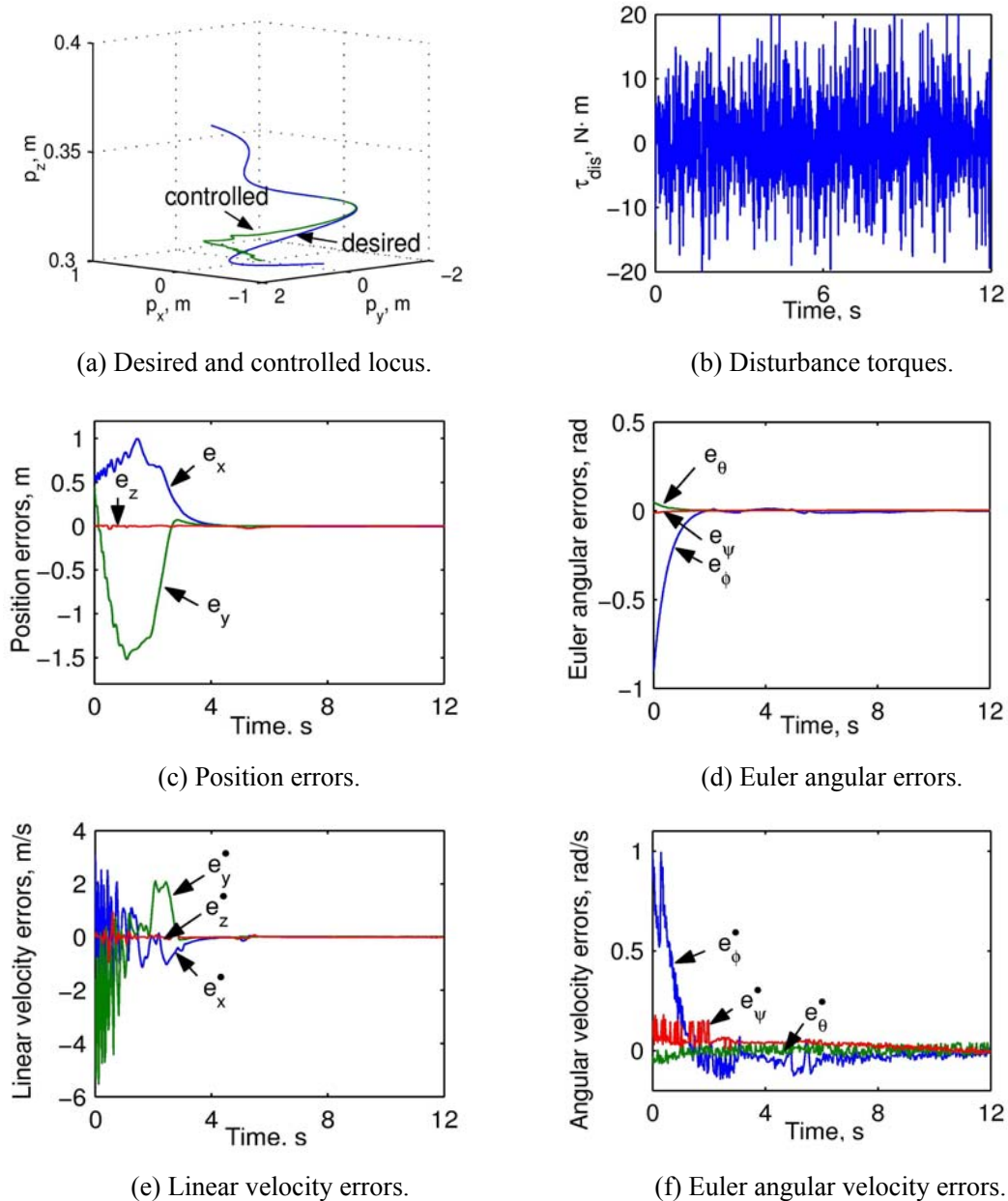


Fig. 4. Simulation results.

moving on a slope. Firstly, an integrated dynamic modeling method is presented, which takes the nonholonomic constraints as well as interactions between the mobile platform and the manipulator into thoroughly consideration. Secondly, an adaptive neural-fuzzy controller is designed for trajectory following of nonholonomic mobile manipulators moving on a slope. Lastly, simulations for a real mobile manipulator composed of a 4-DOF onboard manipulator and a 3-wheeled nonholonomic mobile platform are carried out which demonstrate that the ANFC is robust in case of external disturbances existed. The integrated modeling method and the ANFC can be easily extended to study other nonholonomic systems as well.

## REFERENCES

- [1] Y. Li, Y. Liu, X. Liu, and Z. Peng, "Parameters identification and vibration control in modular manipulators," *IEEE/ASME Trans. Mechatron.*, vol. 9, no. 4, pp. 700-705, Dec. 2004.
- [2] Y. Liu and Y. Li, "Sliding mode adaptive neural-network control for nonholonomic mobile manipulators," *Int. J. Intelligent & Rob. Syst.*, vol. 44, no. 3, pp. 203-224, Nov. 2005.
- [3] L. Sheng and A. Goldenberg, "Neural-network control of mobile manipulators," *IEEE Trans. Neural Netw.*, vol. 12, no. 5, pp. 1121-1133, Sep. 2001.
- [4] Y. Yamamoto and X. Yun, "Effect of the dynamic interaction on coordinated control of

- mobile manipulators,” *IEEE Trans. Rob. Autom.*, vol. 12, no. 5, pp. 816-824, Oct. 1996.
- [5] S. Ge, C. Hang, and L. Woon, “Adaptive neural network control of robot manipulators in task space,” *IEEE Trans. Ind. Electron.*, vol. 44, no. 6, pp. 746-752, Dec. 1997.
- [6] F. Lewis, A. Yegildirek, and K. Liu, “Multilayer neural-net robot controller with guaranteed tracking performance,” *IEEE Trans. Neural Netw.*, vol. 7, no. 2, pp. 388-399, Mar. 1996.
- [7] K. Watanabe, J. Tang, M. Nakamura, S. Koga, and T. Fukuda, “A fuzzy-gaussian neural network and its application to mobile robot control,” *IEEE Trans. Control Syst. Technol.*, vol. 4, no. 2, pp. 193-199, Mar. 1996.
- [8] S. Yi and M. Chung, “A robust fuzzy logic controller for robot manipulators with uncertainties,” *IEEE Trans. Syst., Man and Cybern., Part B: Cybern.*, vol. 27, no. 4, pp. 706-713, Aug. 1997.
- [9] Y. Li and Y. Liu, “Control of a mobile modular manipulator moving on a slope,” *Proc. IEEE Int. Conf. on Mechatron.*, Turkey, pp. 135-140, Jun. 2004.
- [10] C. de Wit, B. Siciliano, and G. Bastin, *Theory of Robot Control*, Springer-Verlag London Limited, 1996.
- [11] L. X. Wang, *Adaptive Fuzzy Systems and Control: Design and Stability Analysis*, Prentice-Hall International, Inc., 1994.
- [12] Y. Li and Y. Liu, “A new task-consistent overturn prevention algorithm for redundant mobile modular manipulators,” *Proc. of IEEE/RSJ Int. Conf. on Intelligent Robots and Systems*, Alberta, Canada, pp. 1563-1568, Aug. 2005.



**Yugang Liu** received the B.Eng. degree from the University of Science and Technology, Beijing, China in 1999, and M.S. degree from the Beijing University of Posts and Telecommunications, Beijing, China in 2002. He is now a Ph.D. candidate in the University of Macau. His research interests include modeling and intelligent control for mobile manipulators, parameter identification and vibration control for modular manipulators.



**Yangmin Li** received the B.Eng. and M.S. degree from the Mechanical Engineering Department, Jilin University, Changchun, China in 1985 and 1988 respectively. He received his Ph.D. from the Mechanical Engineering Department, Tianjin University, Tianjin, China in 1994. He was a Fellow in the United Nations University(UNU/IIST), a visiting scholar in University of Cincinnati, and a Postdoctoral Fellow in Purdue University from 1996 to 1997. He is currently an Associate Professor of University of Macau. His research interests include robotics, mechatronics, control, and automation. He has authored or co-authored about 130 papers in international journals and conferences. He is a Council Member of Chinese journal of Mechanical Engineering, a Senior Member of IEEE, and a member of ASME.